Supporting Information

Protein backbone motions viewed by intraresidue and sequential H^N-H^α residual dipolar couplings

Beat Vögeli, Lishan Yao, and Ad Bax

Laboratory of Chemical Physics, National Institute of Diabetes and Digestive and Kidney Diseases, National Institutes of Health, Bethesda, Maryland 20892.

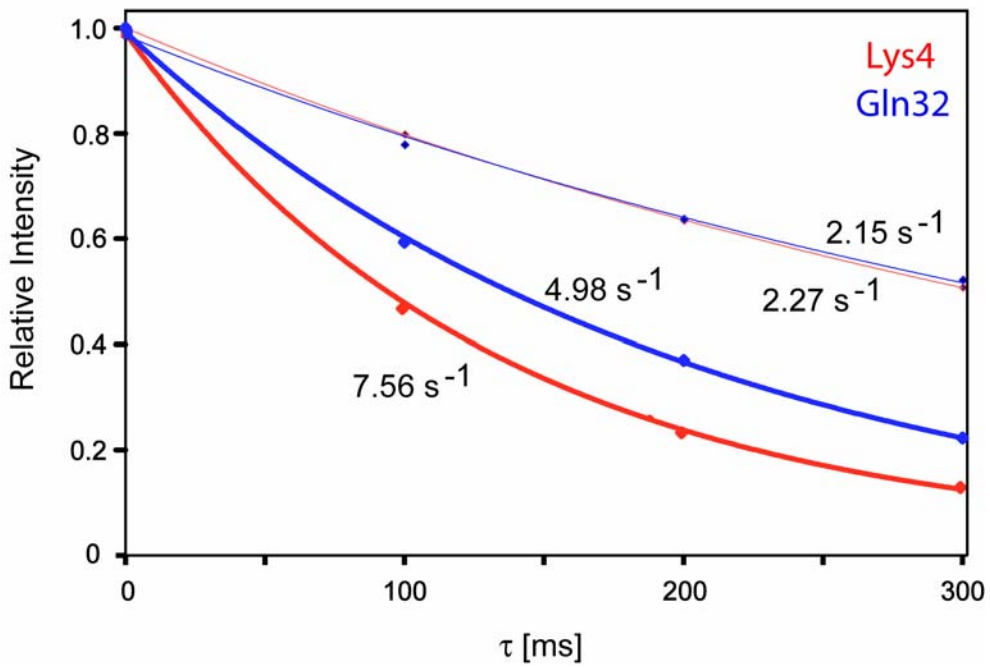

Figure S1. Decay of C^α_z (thin lines) and $2C^\alpha_zH^\alpha_z$ (bold lines). Peak intensities are plotted versus the relaxation time τ for Lys4 (red) and Gln32 (blue). $R_1^{H\alpha}$ is approximated as the difference between $R_1(C^\alpha_z)$ and $R_1(2C^\alpha_zH^\alpha_z)$

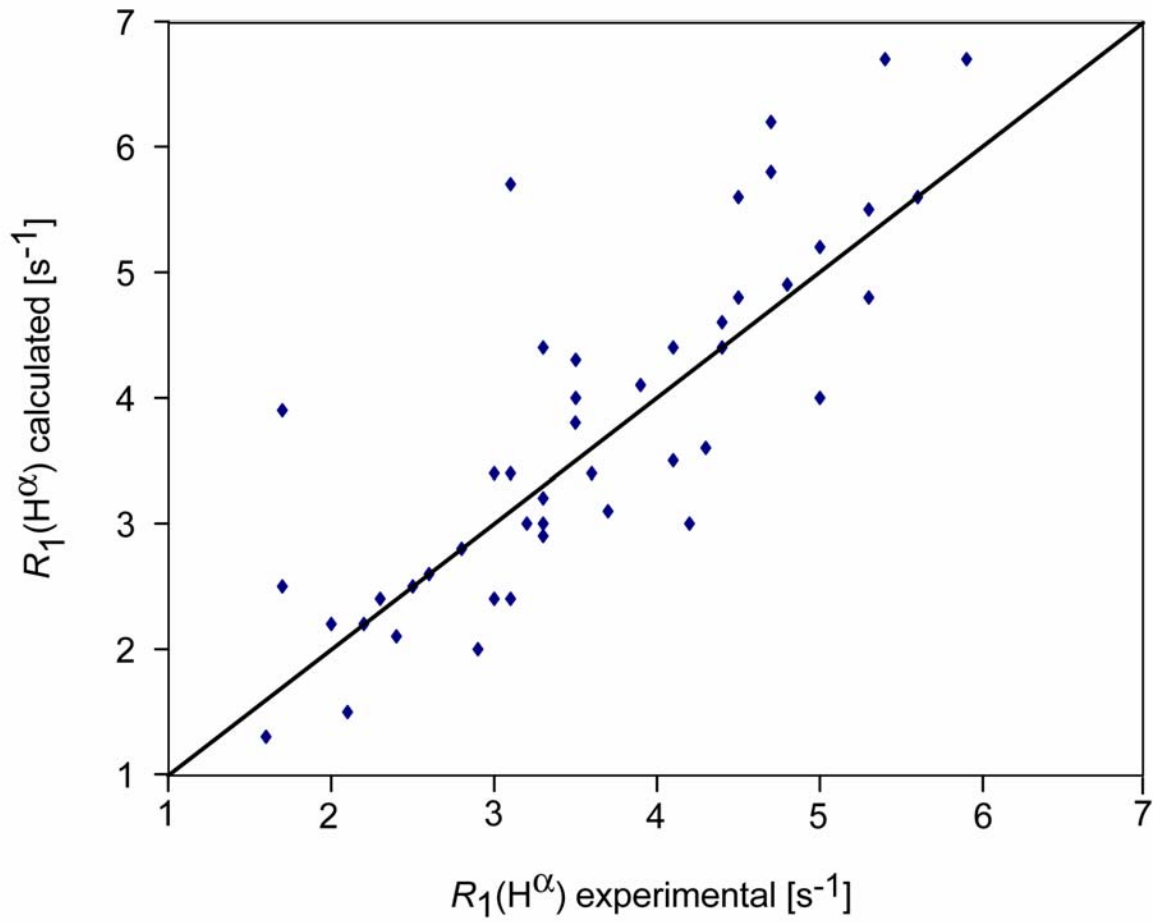

Figure S2. $R_1^{H\alpha}$ relaxation rates calculated on the basis of the 2OED structure of GB3 *versus* experimentally observed values. Calculations of $R_1^{H\alpha}$ only considered J(0) spectral density terms, and assumed isotropic tumbling with a correlation time τ_c = 3.4 ns. Terminal residues, as well as dynamically disordered residues 12, 40 and 41 are excluded. Pearson's correlation coefficient is 0.82.

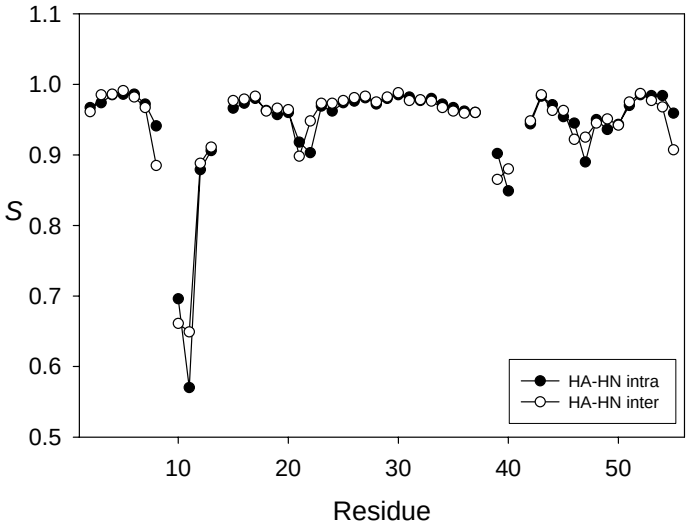

Supplementary Figure 3. Order parameters for H^{α}-H^{N} intra- and sequential inter-residue vectors derived from a 5.6 ns MD simulation. The residue number corresponds to the residue on which H^{α} resides. Gly residues are excluded from the plot. Starting coordinates for the protein atoms in the MD simulation were taken from the GB3 2OED structure. The protein was surrounded by a periodic box of 15 Å (~6500) TIP3P water molecules (Mahoney and Jorgensen, 2000). Na^{+} ions were placed to neutralize the -2 charge of the model system (Pearlman et al., 1995). The parm03 version of the all-atom AMBER force field (Duan et al., 2003) was used for the simulation which was carried out using the SANDER module in *AMBER 8.0* (Case et al., 2004). The SHAKE algorithm (Ryckaert et al., 1977) was used to constrain all bond lengths involving hydrogen atoms, permitting a 2-fs time step. A nonbonded pair list cutoff of 8.0 Å was used, and the nonbonded pair list was updated every 25 steps. The Particle-Mesh-Ewald method (Essmann et al., 1995) was used to evaluate the contributions of the long-range electrostatic interactions. The 5.6 ns MD simulation was performed at constant volume and temperature with the temperature (300 K) controlled by Berendsen's method (Berendsen et al, 1984). The first 1.2 ns of the simulation is treated as the equilibration period and therefore was not included in the order parameter analysis. Each backbone of the trajectory was least squares fitted to the starting structure prior to the order parameter calculation, using $S = \sqrt{\frac{4\pi}{5}\sum_{q=-2}^{2}\left|\left\langle \frac{Y_2^q(\theta,\phi)}{r^3}\right\rangle\right|^2} \Big/ \langle r\rangle^{-3}$, where $Y_2^q(\theta,\phi)$ are the spherical harmonics functions, |…| is the norm and <…> is the trajectory time average.

References

Berendsen, H. H. C.; Postma, J. P. M.; Gunsteren, W. F.; DiNola, A.; Haak, J. R. *J. Chem. Phys.* **1984**, *81*, 3684.

Mahoney, M. W.; Jorgensen, W. L. *J. Chem. Phys.* **2000**, *112*, 8910.

Duan, Y.; Wu, C.; Chowdhury, S.; Lee, M.C.; Xiong, G.; Zhang, W.; Yang, R.; Cieplak, P.; Luo, R.; Lee. T. *J. Comput. Chem.* **2003**, *24***,** 1999-2012.

Pearlman, D. A.; Case, D. A.; Caldwell, J. W.; Ross, W. S.; Cheatham, T. E.; Debolt, S.; Ferguson, D.; Seibel, G.; Kollman, P. *Comput. Phys. Commun*. **1995**, *91*, 1.

Case, D.A.; Darden, T.A.; Cheatham, III, T.E.; Simmerling, C.L.; Wang, J.; Duke, R.E.; Luo, R.; Merz, K.M.; Wang, B.; Pearlman, D.A.; Crowley, M.; Brozell, S.; Tsui, V.; Gohlke, H.; Mongan, J.; Hornak, V.; Cui, G.; Beroza, P.; Schafmeister, C.; Caldwell, J.W.; Ross, W.S.; Kollman, P.A. (2004) AMBER 8, University of California, San Francisco.

Ryckaert, J. P.; Ciccotti, G.; Berendsen, H. J. C. *J. Comput. Phys.* **1977**, *23*, 327.

Essmann, U.; Perera, L.; Berkowitz, M. L.; Darden, T.; Lee, H.; Pedersen, G. L. *J. Chem. Phys.* **1995**, *103*, 8577.

Table S1. Experimental RDCs, $^{1}H^{\alpha}$ longitudinal relaxation rates, "raw" (J+D) couplings and J couplings of GB3.

Residue	$^{1}D_{HN}$ [Hz]	$^{3}D_{HNH\alpha}$ [Hz]	$^{4}D_{HNH\alpha}$ [Hz]	$^{1}D_{C\alpha H\alpha}$ [Hz]	$R_1^{H\alpha}$ [s^{-1}] exp	$R_1^{H\alpha}$ [s^{-1}] calc	$^{3}(D+J)_{HNH\alpha}$ [Hz] raw	$^{3}J_{HNH\alpha}$ [Hz]	$^{4}D_{HNH\alpha}$ [Hz] raw
Gln2					5	5.2			
Tyr3	13.8	1.3	30.6	-34.2	4.2	3.0	10.1	9.8	30.0
Lys4	11.6	-7.6	10.7	-14.8	5.3	5.5	1.6	9.8	9.7
Leu5	-1.5	5.9	15.8	-12.6	5.6	5.6	13.8	9.6	14.2
Val6	7.6	-7.1	4.1	-3.9	4.5	5.6	2.3	9.8	3.5
Ile7	-4.8	4.5	5.5	-10.1	5.4	6.7	12.4	9.6	4.7
Asn8	10.2	-4.9	13.7	-13.1	3.1	5.7	4.6	9.9	12.0
Gly9	-17.3		-8.5			5.5			-8.0
Lys10	10.6	-3.2		-24.2	2.2	2.2	1.6	5.0	
Thr11	13.0	-6.3	-4.1	-24.5	1.7	2.5	3.8	10.3	-3.8
Leu12		7.2	0.3	-12.8	3.5	4.3	14.0	7.8	0.2
Lys13	10.5		0.3		3.9	4.1		9.9	0.3
Gly14	5.3		16.8			2.7			15.8
Glu15	5.5	-6.1		6.3	4.1	4.4	2.0	8.4	
Thr16	7.9	4.6	4.6	11.5	2.9	2.0	10.3	6.7	4.0
Thr17	13.6	-7.4	0.2	-7.9	5.3	4.8	1.0	8.9	0.2
Thr18	16.9	-3.3	-0.8	-8.0	3.1	2.4	3.1	6.7	-0.6
Lys19	14.3	-5.8	-0.3	-32.8	4.4	4.6	3.0	9.4	-0.3
Ala20	12.1	-6.6	-12.3	-18.9	3.1	3.4	0.5	7.2	-11.1
Val21	13.7	-4.4	-12.5	29.3	2.3	2.4	-0.1	4.3	-11.9
Asp22	12.6	-7.3	6.9	-18.6	3.3	3.0	-0.7	6.3	6.3
Ala23	16.7	-5.0	19.1	-21.6	3	3.4	-1.7	3.0	18.2
Glu24	2.9	6.6	-3.0	45.2		3.1	9.8	3.9	-2.8
Thr25		-4.8	4.5	-4.1	2.6	2.6	0.5	5.4	4.1
Ala26	11.9	-6.7	-1.7	-9.1	3.1	3.4	-2.1	4.4	-1.6
Glu27			2.6		3.7	3.1			2.4

Lys28	-2.5	1.4	-2.4	58.4	3.3	2.9	4.5	3.6	-2.2
Ala29	3.3	-6.9	4.5	-30.3	2.5	2.5	-2.0	4.8	4.2
Phe30	11.8		-2.0		5.9	6.7		4.8	-1.9
Lys31	4.8	7.1		6.3	4.1	3.5	10.0	4.1	2.7
Gln32	-7.7		2.6		2.8	2.8	1.4	5.2	2.2
Tyr33	4.9		2.3	-24.5	3	2.4	-7.4	3.2	2.1
Ala34	10.7	0.7	0.9	-24.8	3.6	3.4	3.9	3.6	0.8
Asn35	0.1	6.9	-2.7	48.1	2.1	1.5	10.2	3.7	-2.5
Asp36	-2.4		5.1	-11.2	1.6	1.3		3.6	4.8
Asn37			-3.6	-35.9	1.7	3.9	7.2	9.3	-3.5
Gly38	7.3		1.2			1.9			1.1
Val39	-16.9				3.3	4.4	13.4	8.9	
Asp40				16.1	4.4	2.5	3.7	8.4	1.2
Gly41			-8.8			4.3			-7.8
Val42	12.7	-6.4		-21.9	3.5	4.0	2.0	8.7	
Trp43	1.6	5.2	12.6	-11.2	4.3	3.6	12.6	8.7	11.5
Thr44	6.6	-6.3	-2.7	-15.9	3.3	3.2	2.4	8.9	-2.3
Tyr45	-0.7	8.6	11.5	-14.8	4.8	4.9	16.1	8.8	10.5
Asp46	8.9	-7.1	4.8	-4.1	3.2	3.0	2.5	9.8	4.2
Asp47	-12.1	7.3	4.8	-26.5	3.5	3.8	10.6	4.0	4.3
Ala48	-24.3	10.7	-3.4	20.6	2	2.2	14.7	4.3	-3.2
Thr49	-26.4	5.3	-1.5	47.7	2.4	2.1	14.9	10.1	-1.5
Lys50	8.3	-12.6	-1.3		4.7	6.2	-5.1	7.0	-1.2
Thr51	11.3	-7.9	2.3	-12.0	4.7	5.8	2.0	10.3	2.0
Phe52	-3.0	4.1	9.8	-12.6	5	4.0	12.2	9.5	8.8
Thr53	5.5	-6.4	13.7	-5.1	4.4	4.4	2.8	9.7	12.2
Val54	1.4	2.7	7.0	-12.5	4.5	4.8	11.5	10.0	6.2
Thr55	10.7	-5.4	19.5	-10.2	2.4	4.3	4.3	9.9	18.3
Glu56		2.0	4.8	-21.0		3.3	9.5	8.3	4.6

Table S2. Effective order parameters and orientation of the principal axis system of the alignment tensor relative to the 2OED coordinates, obtained from fits to eq 5, when considering each coupling type separately.

Coupling type	# res	$S^{eff}_{xx,mol}$ [10^{-4}]	$S^{eff}_{yy,mol}$ [10^{-4}]	$S^{eff}_{zz,mol}$ [10^{-4}]	α	β	γ	rmsd [Hz]	*r*
$^1D_{HN}$	47[a]	5.80	7.61	-13.41	59.1°	82.7°	172.5°	0.76	0.997
$^3D_{HNH\alpha}$	41	5.34	7.84	-13.19	56.6°	77.6°	171.2°	0.99	0.987
$^4D_{HNH\alpha}$	46[b]	5.21	6.85	-12.06	59.3°	83.2°	165.9°	1.92	0.961

[a] Residues 12, 40 and 41 excluded. [b] Residue 40 excluded.
[b] Pearson's correlation coefficients, *r*, are higher than the corresponding values in Table 1, main text, because a five-parameter SVD fit is used to correlate experimental data to the 2OED structure.

Table S3. Scalar products between the effective alignment tensors obtained from $^1D_{HN}$ and D_X, and tensor norms standardized to $^1D_{HN}$ tensor norm obtained from fits to 2OED.

coupling type X	# res	scalar product	angle	relative tensor norms
$^1D_{HN}$	47[a]	1	0°	1
$^3D_{HNH\alpha}$	41	0.985	10.1°	0.986
$^4D_{HNH\alpha}$	46[b]	1.000	1.4°	0.900

[a] Residues 12, 40 and 41 excluded. [b] Residue 40 excluded.

Table S4. Order parameters and orientation of the principal axis system of the alignment tensor relative to an ensemble of 160 conformers (best fit to one another using heavy backbone atoms) obtained from fits to eq 1, when considering each coupling type separately

Coupling type	# res	$S_{xx,mol}$ [10^{-4}]	$S_{yy,mol}$ [10^{-4}]	$S_{zz,mol}$ [10^{-4}]	α	β	γ	rmsd [Hz]	*r*
$^1D_{HN}$	47[a]	6.14	7.96	-14.10	60.1º	89.5º	167.2º	0.54	0.999
$^3D_{HNH\alpha}$	41	5.12	7.95	-13.07	58.3º	84.5º	171.1º	0.99	0.987
$^4D_{HNH\alpha}$	46[b]	5.17	7.37	-12.54	59.9º	89.6º	169.3º	0.99	0.994

[a] Residues 12, 40 and 41 excluded. [b] Residue 40 excluded.
[b] Pearson's correlation coefficients, *r*, are higher than the corresponding values in Table 1, main text, because a five-parameter SVD fit is used to correlate experimental data to the 2OED structure.

Table S5. Scalar products between the tensors obtained from $^1D_{HN}$ and D_X with tensor norms standardized relative to the $^1D_{HN}$-derived tensor, obtained from fits to an ensemble of 160 conformers.

coupling type X	# res	scalar product	angle	relative tensor norms
$^1D_{HN}$	47[a]	1	0º	1
$^3D_{HNH\alpha}$	41	0.985	10.0º	0.931
$^4D_{HNH\alpha}$	46[b]	0.997	4.0º	0.892

[a] Residues 12, 40 and 41 excluded. [b] Residue 40 excluded.

Table S6. Scalar products between the tensors obtained from fits to the 2OED[a] structure and the ensemble of 160 conformers.

coupling type	scalar product (ensemble,2OED)	angle	norm(ensemble)/ norm(2OED)
$^{1}D_{\mathrm{HN}}$	0.995	6.0°	1.051
$^{3}D_{\mathrm{HNH\alpha}}$	0.998	3.8°	0.993
$^{4}D_{\mathrm{HNH\alpha}}$	0.993	6.6°	1.042

[a] The heavy backbone atoms of 2OED and the ensemble were aligned.